TYC 1417-891-1 and TYC 1478-742-1: Eclipsing variable stars. The Gaia EDR3 and TESS photometric data.

K. K. Gigoyan *, K. S. Gigoyan †, and G.R. Kostandyan ‡

INAS RA V. Ambartsumian Byurakan Astrophysical Observatory (BAO), Byurakan 0213, Aragatzotn Province, Armenia

Abstract

Based on the TESS (Transiting Exoplanet Survey Satellite) phase dependent light curves, we confirm the eclipsing type variability nature for two G – type dwarfs: TYC 1417-891-1 and TYC 1478-742-1. Both objects show EA (Algol – type) light curves morphology. Orbital period for TYC 1417-891-1 is P $\approx$ 8.0 day and for TYC 1478-742-1, P $\approx$ 13.6 day. We present Gaia EDR3 and TESS catalogue important physical parameters as well as LAMOST spectra. Both objects are relatively bright and are located at a distance of 260.59 ($\pm$3.21) pc (TYC 1417-891-1) and 117.42 ($\pm$0.74) pc (TYC 1478-742-1). The TESS light curve of TYC 1478-742-1 show also flares as well. We discuss possible nature of the secondary and faint objects around these stars.

Keywords: *variables, eclipsing variables: TESS and Gaia data.*

1. Introduction

Variable stars are an important and dynamic area of modern astronomical research. Brightness variability is seen for most stars. Variability provides extra observational information (periods, amplitudes, etc.) which can be used to determine physical parameters such as a mass, radius, luminosity, and rotation rates. These parameters can be used to deduce some characteristics of the stars. The study of variability allows us to directly observe changes in the stars: both the rapid and sometimes violent changes associated especially with stellar birth and death, and also changes associated with most stellar evolution. Variable stars are classified as several broad classes: pulsating, eclipsing, rotating, eruptive, cataclysmic, and many other. Each class of variable stars is divided into several subclasses. More detail, the improved system of variability classification is presented by authors of the "General Catalogue of Variable Stars"(GCVS) (accessed via https://www.sai.msu.su/gcvs/gcvs/vartype.htm for details; Samus' et al., 2017). Historically, there are three basic classes of eclipsing variables, based solely on the overall light curve shape, EA (Algol), EB (Beta Lyrae), and EW (W Ursae Majoris) - types. An overview of variable stars, in general, the techniques for discovering and studying variable stars, and description of the main types of variable stars are presented also in the book of Percy (2007) and in papers by Drake et al. (2014, 2017). Correct class determination of the variables can be very important for studies of stellar populations. Some types of variable stars, such as RR Lyrae stars and Cepheids, are excellent tools to study our Galaxy. Long period variables (LPV, $\triangle$V $\geq$ 2.5 mag., or Miras), which are Asymptotic Giant Branch (AGB) stars, are also very important distance indicators (Whitelock et al., 2008).

The number of discovered variable stars increases dramatically, particularly in the last two decades. Catalogs of about 47 055 periodic variables in Northern and 37 745 in Southern hemisphere were published by Drake et al. (2014, 2017), based on the Catalina Sky Survey (CSS). Data for near 116000 variables were presented by Christy et al. (2023), based on All – Sky Automated Survey for Supernovae (ASAS – SN) observations. A new catalogue of 6330 eclipsing variables was presented by Malkov et al. (2006). A new version of the catalogue of eclipsing variables is presented by Avvakumova et al. (2013). This catalogue contains parameters and morphological types of light curves for some 7200 stars. Eclipsing binaries, from the surveys ASAS, NSVS, and LINEAR are analyzed by Lee (2015). An updated catalog of 4680 northern

*karengigoyan@bao.sci.am, Corresponding author
†kgigoyan@bao.sci.am
‡kostandyan@bao.sci.am

doi: https://doi.org/10.52526/25792776-23.70.1-60

Table 1. TESS observations of two stars from she MAST

Star	TESS Target Name	Data of Observations	Exposure length (sec)
TYC 1417-891-1	88063457	2021-11-07	120
TYC 1417-891-1	88063457	2022-01-24	120
TYC 1478-742-1	462578519	2022-04-23	120

eclipsing binaries with Algol – type light curve morphology was presented by Papageorgiou et al. (2018). Data for near 220000 variables have been identified in the ASAS-SN survey (Jayasinghe et al., 2020). Recently, more than 40000 eclipsing binary candidates identified by the ASAS – SN, were also presented by Rowan et al. (2022). These new results, undoubtedly, are very important for the further versions of the GCVS (Samus' et al., 2017).

TESS (Transiting Exoplanet Survey Satellite, Ricker et al., 2014) is an all – sky space based mission designed to search for planets transiting around nearby dwarfs. Phase dependent light curves for all FBS M dwarfs (Gigoyan et al., 2023) were analyzed using the Presearch of Data Conditioning Simple Aperture Photometry (PDCSAP) at the Mikulski Archive for Space Telescopes (MAST, access via https://mast.stsci.edu/portal/Mashup/Clients/Mast/Portal.html/). During the analysis of the TESS data, our attention was drawn there on phased light curves of Target Numbers 88063457 and 462578519. These two objects were associated in SIMBAD (http://simbad.u-strasbg.fr) astronomical data base with the proper motion stars TYC 1417-891-1 ((RA = $09^h51^m39.93^s$, DEC = $20°12'23.8''$) and TYC 1478-742-1 (RA = $14^h48^m28.91^s$, DEC = $+15°05'12.3''$), coordinates are for Equinox J2000.0) without information on spectral types and variability. We classified these two objects as EA (Algol – type) eclipsing binaries and analyzed their TESS phase dependent light curves. The purpose of this paper is to present most important physical parameters from the Gaia EDR3 and TESS catalogues. We also discuss possible nature of the secondary and faint objects around these eclipsing variables. This paper is structured as follows. In Section 2 of this paper, we present the TESS light curves for TYC 1417-891-1 and TYC 1478-742-1. Section 3 presents LAMOST moderate-resolution spectra for these two objects. Photometric data, cross-correlations with Gaia EDR3 and TESS catalogues and important physical parameters are considered in Section 4. Finally, in Section 5, we discuss the results obtained for these two stars, and we provide the concluding remarks.

2. TESS light curves

The Transiting Exoplanet Survey Satellite (TESS, Ricker et al., 2014) is an ongoing NASAs Astrophysics Explorer Mission designed to detect exoplanets around the nearest M dwarfs, ideal to follow – up observations for further characterization. TESS was launched on 2018 April 18, and the TESS Prime Mission (PM) ran from 2018 July 25 to 2020 July 4. During its 2 years PM, TESS observed $\sim$ 73% of the sky across 26 observing "Sectors", resulting in observing times ranging from $\sim$ 1 month near the ecliptic to $\sim$ 1 year near the poles. It monitored bright stars with a 2 minutes short cadence and provided full-frame images every 30 minutes. The wide red bandpass of the TESS cameras (600-1000 nm) makes TESS capable of detecting Earth and super – Earth – sized exoplanets ($R \leq 1.75 R_{\odot}$) transiting M dwarfs. TESS observed TYC 1417-891-1 twice: during its second year of operation in its high – cadence, two minutes cadence mode in Sector 45 (2021 June, and December), and also in Sector 46 (2021 March, and 2022 January). TESS observed TYC 1478-742-1 in 23 April 2022, in Sector 51, as well in two – minute cadence mode. Table 1 presents TESS observational data for TYC 1417-891-1 and TYC 1478-742-1 from the MAST.

We downloaded the PDCSAP light curves for these stars from the MAST using the lightkurve package (Barentsen et al., 2019).

Figure 1 and 2 shows TESS SAP (Simple Aperture Photometry) original light curves of TYC 1417-891-1 and of TYC 1478-742-1 from Sectors 46 and 51.

Both objects (Fig. 1 and 2) show TESS light curves with almost flat maxima. We classify both objects as EA (Algol – type) eclipsing variables. For TYC 1417-891-1 both minimum (primary and secondary) are very well expressed on TESS phase dependent light curves. For TYC 1478-742-1 there is a gap in the TESS data when the primary eclipse would be appeared. The TESS light curve of this object also shows flares. We used Box Least Squares (BLS; Kovács et al., 2002) periodogram analysis method to estimate the orbital periods. We determined the orbital period P $\approx$ 8 day for TYC 1417-891-1 and near P $\approx$ 13.6

doi: https://doi.org/10.52526/25792776-23.70.1-60

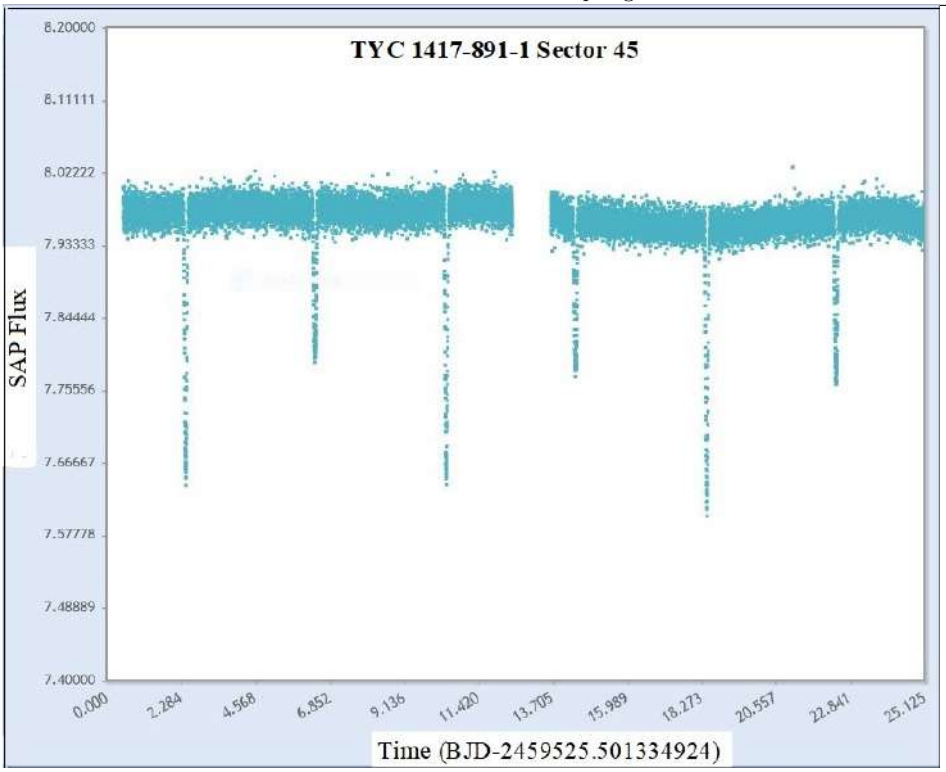

Figure 1. The TESS SAP original flux time series photometry of TYC 1417-891-1 from Sector 46. The X-axis show the time in Barycentric Julian Days (BJD) and Y-axis shows the normalized TESS SAP flux.

Table 2. LAMOST Data for Two Stars

Star	LAMOST Designation	Obs. Identifier	Data of Obs	Subclass
TYC 1417-891-1	J095139.94+201223.3	286412016	2014-12-26	G5V
TYC 1478-742-1	J144828.92+150512.2	350111159	2015-05-26	G8V

days for TYC 1478-742-1. Important note, both objects have monitored photometric data in Catalina Sky Survey (Drake et al. (2014, 2017) data base, see also http://nesssi.cacr.caltech.edu/DataRelease/). Their CSS identifiers are consequently CSS J095139.9+201222 and CSS J144828.9+150511. The CSS light curves do not present the primary and secondary eclipses for both objects as well, such as TESS light curves. Only the CSS phase dependent light curve for TYC 1478-742-1 shows flare with amplitude $\triangle m_v \approx 0.75$mag. We want to note also, that photometric data for TYC 1417-891-1 is available in AAVSO VSX database (https://www.aavso.org/vsx/), with name VSSP J095139.94+ 201223.2, Period = 8.00405 days, Mag. range = 11.325(±0.08) in V-band, spectral type G6, and variability type EA+UV (UV – eruptive variables of the UV Ceti types). There are no data for the second object TYC 1478-742-1 in AAVSO VSX data base.

3. LAMOST spectra

Moderate – resolution CCD spectra for TYC 1417-891-1 and TYC 1478-742-1 were secured by LAMOST (Large Sky Area Multi-Object Fiber Spectroscopic Telescope) observations (Cui et al. (2012), spectrum is available online at http://dr7.lamost.org./search/). In Table 2, we provide information on LAMOST spectral observations.

Figure 3 present the LAMOST moderate-resolution spectra for TYC 1417-891-1 and TYC 1478-742-1.

4. Photometric Data. Physical Parameters.

4.1. Gaia EDR3 Data

Gaia EDR3 (Gaia Collaboration et al., 2021) provides high-precision astrometry, three-band photometry, radial velocities, effective temperatures, and information on numerous astrophysical parameters for

doi: https://doi.org/10.52526/25792776-23.70.1-60

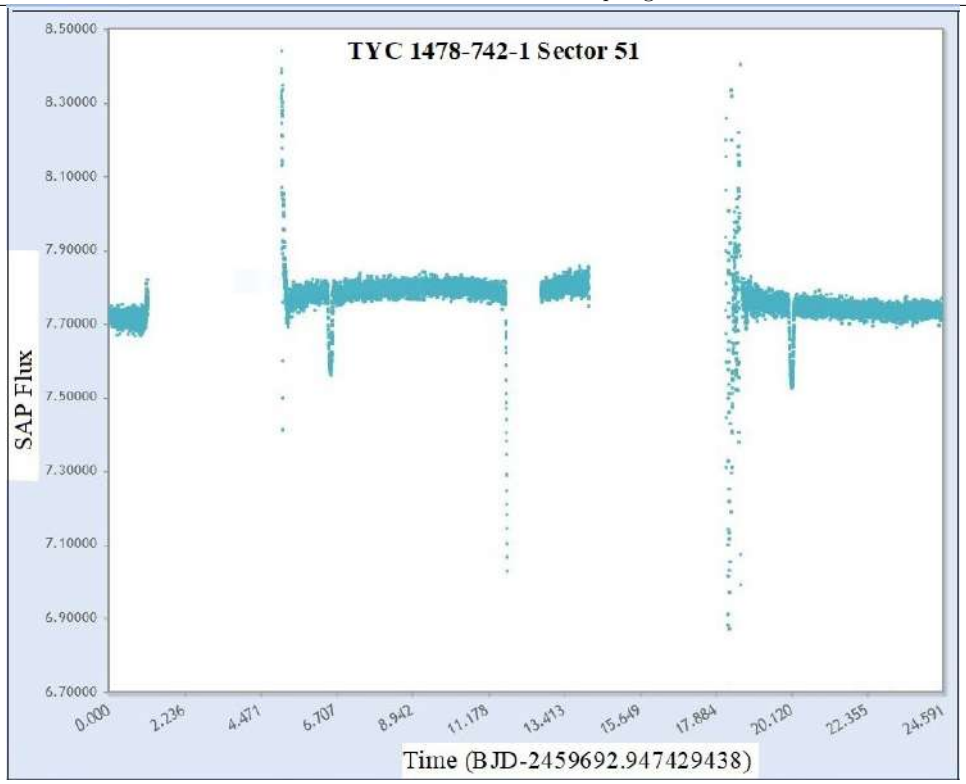

Figure 2. The TESS SAP original flux time series photometry of TYC 1478-742-1 from Sector 51. The X and Y axis description is the same, as in Figure 1.

Table 3. LAMOST Data for Two Stars

Star	Gaia EDR3 Name	G-mag	BP mag	BP-RP mag.	R(pc)
TYC 1417-891-1A	627614504288922112	11.089	11.448	0.885	261.97
B	627614504288958464	17.292	18.707	2.658	275.67
TYC 1478-742-1A	1186217744648523008	11.265	11.738	1.117	124.17
B	1186217740354601600	17.648	17.837	0.967	1943.05

approximately 1.8 billion sources brighter than G = 21.0 magnitude. Gaia EDR3 database gives data for two objects in 10 arcsec. search radius around positions of TYC 1417-891-1 and TYC 1478-742-1. We used the distance information for both objects derived from Gaia EDR3 by Bailer-Jones et al. (2021) . In Table 3 we give some important Gaia EDR3 data for TYC 1478-742-1 and for TYC 1417-891-1 in 10 arcsec. search radius (A - for the bright, primary source and B-for the secondary faint source).

4.2. TESS Photometric Data

NASAs TESS is an all–sky space–based mission designed to search for planets transiting around nearby dwarfs (Ricker et al., 2014). TESS completed its PM July 2020 and now it is in its extended mission. We have cross–matched these two dwarfs with the TESS Input Catalog, Version 8.2 (TIC V8.2; Paegert et al., 2021), giving the important physical parameters for stars, parallaxes, proper motions, TESS T- magnitudes, temperatures, masses, and luminosities in solar units Stassun et al. (2018). This catalogue also gives data for two objects in 10 arcsec. search radius around positions of TYC 1417-891-1 and TYC 1478-742-1. Table

Table 4. TIC v8.2 Catalog Data for TYC 1478-742-1 and for TYC 1417-891-1

Star	TIC Number	2MASS J-H color	2MASS H-K color	Rad (R_{Sun})	Mass (M_{Sun})	Lum (L_{Sun})	T_{Eff} (K)	Dist (pc)
TYC 1417-891-1A	88063457	0.351	0.056	1.443(±0.405)	1.010(±0.126)	1.949(±0.018)	5678	261.20(±3.21)
B	88063458	0.644	0.291	0.405(±0.017)	0.397(±0.025)	0.018(±0.005)	3348	271.16(±9.81)
TYC 1478-742-1A	462578519	0.454	0.111	0.727(±0.037)	0.884(±0.107)	0.348(±0.009)	5200	117.42(±0.749)
B	1100510113							1981.76(±446.77)

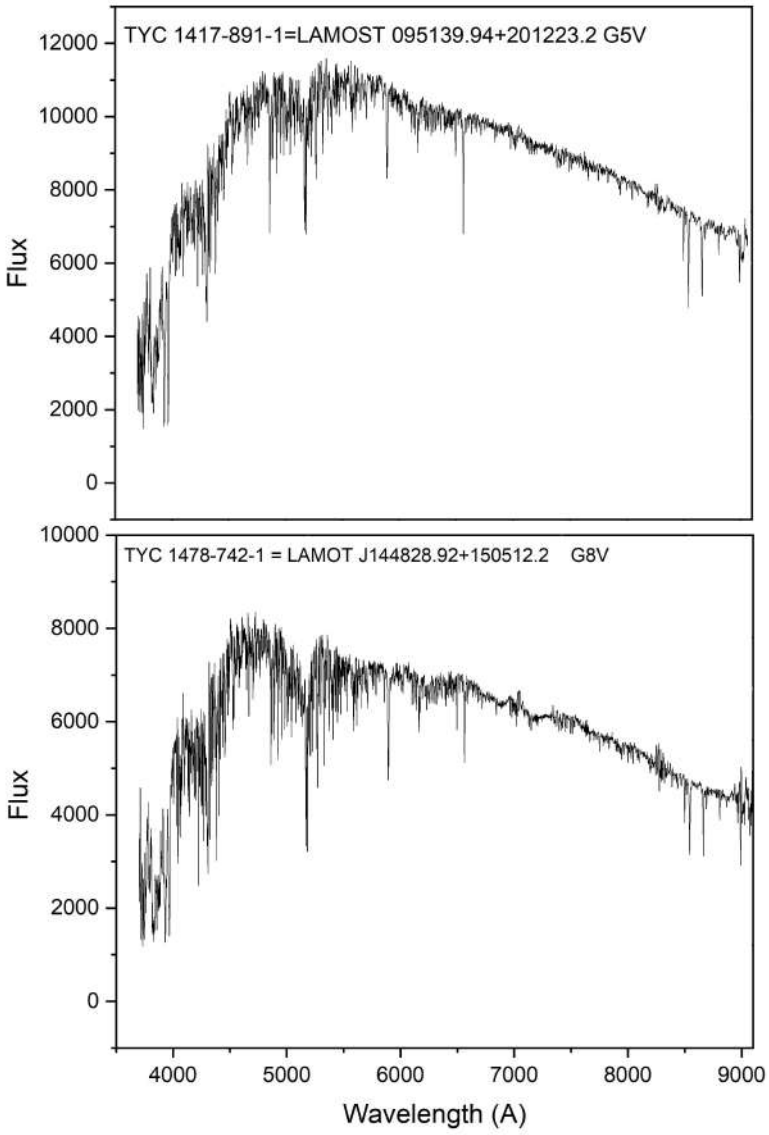

Figure 3. LAMOST moderate-resolution CCD spectra for TYC 1417-891-1 and TYC 1478-742-1 in the range 3900-9100 Å.

4 includes other very important physical parameters from the TIC, V8.2 Paegert et al. (2021). The bright and faint components are noted as A and B, as in Table 1.

5. Discussion and conclusions. Further works.

EA (Algol-type) eclipsing variables are binaries (semi-detached systems) with spherical or slightly ellipsoidal components. Various sub-classes of semi-detached systems can be separated (for example hot and cool Algol-types). For cool semi–detached systems the component is of types G and later (see paper by Malkov et al. (2006) for more detail). With the help of standard image visualization and analysis is software SAOImage ds9, we search STScI Digitized Sky Survey POSS2 and POSS1 images (online at https://archive.stsci.edu/cgi-bin/dss_form/) around position of each object. Obviously, the DSS2 I (infrared) and B (blue) direct images of this two primary and bright objects A are elongated. Figure 4 presents DSS2 I finder chart for TYC 1417-891-1 (the primary bright star is circled as A, and the secondary faint object as B, as it is presented in Table 3 and 4 for this objects). Such images are very characteristic for numerous of nearby dwarf binary systems (particularly such as GJ 2069, which is also eclipsing binary, see more detail López-Morales & Clemens (2004). The Gaia EDR3 catalog gives proper motion (pm) value = 22.920 mas/yr for second faint object B. The TIC V8.2 (Paegert et al., 2021) catalogue distances are consequently r = 261.201 (± 3.218) pc and r = 271.164 (±9.812) pc for TYC 1417-891-1 A and B components (Table 4). If these objects (circled as A and B in Figure 4 are gravitation- ally bound, i. e. they are physical

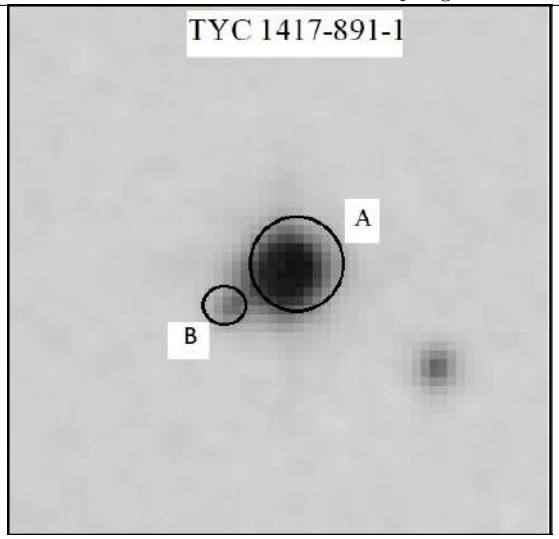

Figure 4. POSS2 I finder chart for TYC 1417-891-1 (A for bright and B for faint and very close object) taken in 1996. Obviously, the bright star A is elongated. Field is ∼ 1.5 arcmin. x 1.5 arcmin.

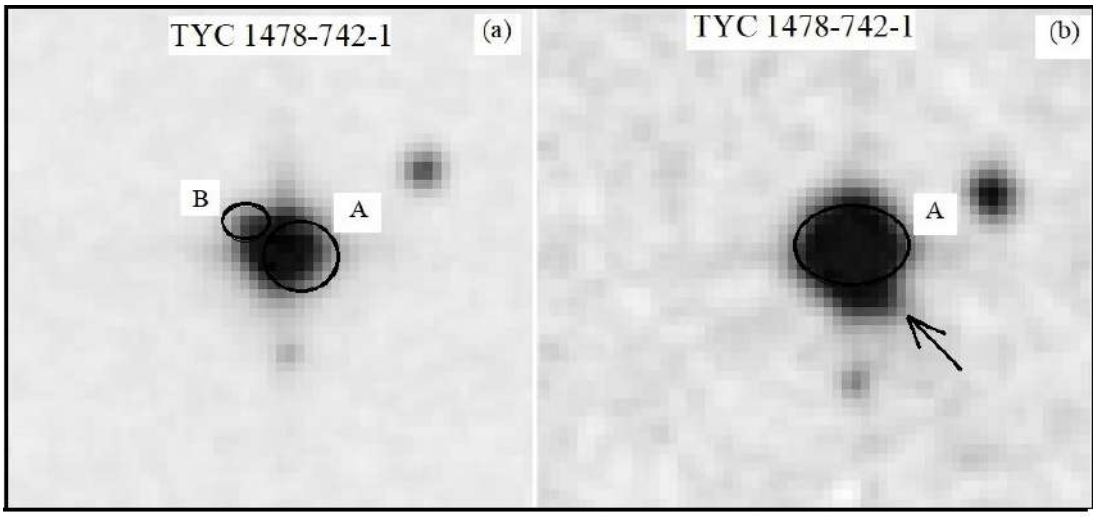

Figure 5. Figure 5(a) POSS2 blue image of TYC 1478-742-1 taken in 1996. Circled (B) is the very close and faint object existing in Gaia EDR3 and TESS catalogues. Figure 5 (b) is the POSS1 B image of the same object. Arrow indicate the very faint object in south-east direction. For this object there are no data in Gaia EDR3 and TESS catalogues. Field is 2 arcmin × 2 arcmin.

companions at the same distances, therefore their G-band absolute magnitudes can be obtained M(G) = +6.0 for bright A star and M(G) = +10.20 for faint object B. Such parameters for faint object (M(G) = +10.20, BP-RP = 2.658 mag., T_{eff} = 3348 K) placed it in red dwarfs sequence on Hertzsprung-Russeill Diagram (HRD, see Fig. 5 by Babusiaux et al. (2018) and is typical for M4-M5 subtype dwarfs (Cifuentes et al., 2020). As a supplement, 2MASS (Skrutskie et al., 2006) J-H = 0.644 and H-K = 0.291 Near-Infrared (NIR) colors for this object (Table 4) also indicate the belonging to the group of dwarf M stars (see NIR JHK colors of M dwarfs in papers by Bessell (1991), Bessell & Brett (1988)). Most probably, TYC 1417-891-1 is a triple system, with two very close and bright stars, having practically equal magnitudes, and third component as M dwarf.

The primary and bright object A for the second object TYC 1478-742-1 is also elongated on POSS2 I and B finder charts. Gaia EDR3 and TESS data bases gives very different distance values for bright A and for faint B sources ($r \approx 1980$ pc for faint object B). In figure 5 (a) and (b) we present POSS2 B (a)(for Equinox J2000) and POSS1 B (b)(for Equinox B1950) direct images for object TYC 1478-742-1. Meanwhile, Gaia EDR3and TESS catalogs show proper motion for object B (the Gaia EDR3 catalogue data is 22.92 mas/yr for proper motion). On DSS1 B (equinox B1950) chart we see very faint object, which we indicate by arrow (Figure 5 (b)). This object is not visible on DSS2 B and I chart (Figure 5(a)). We note, that the

doi: https://doi.org/10.52526/25792776-23.70.1-60

scaling factor of DSS2 is 1.6 time better than DSS1. This point needs to study more detail in the future. For this faint object there are no 2MASS JHK photometric data and Gaia EDR3 BP-RP = 0.967 mag. The TESS light curve shows flares.

High-spatial-resolution CCD imaging and speckle interferometry in the future allow us to study the nature of the companions around these objects in more detail. Our conclusions can be summarized as follows:

(a) Based on TESS phase dependence light curves, we confirm EA-type eclipsing variability nature for objects TYC 1417-891-1 and TYC 1478-742-1 consequently with orbital period $P \approx 8.0$ day and $P \approx 13.6$ day. EA-variability type for TYC 1478-742-1 we present for the first time.

(b) Using Gaia EDR3 and TESS data bases, we present some very important physical characteristics for two objects, such as, mass, radius, luminosities, effective temperatures, etc. They are spectral subtypes G5V (TYC 1417-891-1) and G8V (TYC 1478-742-1) and consequently at a distances 261 pc and 124 pc.

(c) Most probably TYC 1417-891-1 present a triple system having two bright and very close companions, and third very faint companion as M dwarf.

Acknowledgements

This work is supported by ERASMUS+2019-1FRO-KA 107-061818. KKG and KSG are grateful to Administration of OVSQ Observatory an LATMOS Laboratory (France) for organizing their visit to LATMOS Laboratory during June and July 2022. This research has made use of the VizieR catalogue access tool, CDS, Strasbourg, France., and Two Micron All-Sky Survey, which is a joint project of the University of Massachusetts and the Infrared Processing and Analysis Center, funded by NASA and NSF. We used LAMOST telescope spectra. The LAMOST is a National Major Scientific project build by the Chinee Academy of Sciences. This work has made use of data from European Space Agency (ESA) mission Gaia(https://cosmos.esa.int/gaia/). This paper includes data collected by the TESS mission, which are publicly available from the Mikulski Archive for Space Telescopes (MAST).

We thank Prof. Michelle Kunimoto and Oleg Malkov for helpful comments and suggestions. Authors thank also our anonymous Referee for valuable suggestions and contributions.

References

Avvakumova E. A., Malkov O. Y., Kniazev A. Y., 2013, Astronomische Nachrichten, 334, 860

Babusiaux C., van Leeuwen F., Barstow M. A., Jordi C., Zucker S., Zurbach C., Zwitter T., 2018, Astron. Astrophys. , 616, A10

Bailer-Jones C. A. L., Rybizki J., Fouesneau M., Demleitner M., Andrae R., 2021, Astron. J. , 161, 147

Barentsen G., et al., 2019, KeplerGO/lightkurve: Lightkurve v1.6.0, Zenodo, doi:10.5281/zenodo.3579358

Bessell M. S., 1991, Astron. J. , 101, 662

Bessell M. S., Brett J. M., 1988, Publ. Astron. Soc. Pac. , 100, 1134

Christy C. T., et al., 2023, Mon. Not. R. Astron. Soc. , 519, 5271

Cifuentes C., et al., 2020, Astron. Astrophys. , 642, A115

Cui X.-Q., et al., 2012, Research in Astronomy and Astrophysics, 12, 1197

Drake A. J., et al., 2014, Astrophys. J. Suppl. Ser. , 213, 9

Drake A. J., et al., 2017, Mon. Not. R. Astron. Soc. , 469, 3688

Gaia Collaboration et al., 2021, Astron. Astrophys. , 650, C3

Gigoyan K. S., Sarkissian A., Kostandyan G. R., Gigoyan K. K., Meftah M., Bekki S., Azatyan N., Zamkotsian F., 2023, pasa, 40, e023

Jayasinghe T., et al., 2020, Mon. Not. R. Astron. Soc. , 491, 13

Kovács G., Zucker S., Mazeh T., 2002, Astron. Astrophys. , 391, 369

Lee C.-H., 2015, Mon. Not. R. Astron. Soc. , 453, 3474

López-Morales M., Clemens J. C., 2004, Publ. Astron. Soc. Pac. , 116, 22

Malkov O. Y., Oblak E., Snegireva E. A., Torra J., 2006, Astron. Astrophys. , 446, 785

Paegert M., Stassun K. G., Collins K. A., Pepper J., Torres G., Jenkins J., Twicken J. D., Latham D. W., 2021, arXiv e-prints, p. arXiv:2108.04778

Papageorgiou A., Catelan M., Christopoulou P.-E., Drake A. J., Djorgovski S. G., 2018, Astrophys. J. Suppl. Ser. , 238, 4

Percy J. R., 2007, Understanding Variable Stars

Ricker G. R., et al., 2014, in Oschmann Jacobus M. J., Clampin M., Fazio G. G., MacEwen H. A., eds, Society of Photo-Optical Instrumentation Engineers (SPIE) Conference Series Vol. 9143, Space Telescopes and Instrumentation 2014: Optical, Infrared, and Millimeter Wave. p. 914320 (arXiv:1406.0151), doi:10.1117/12.2063489

Rowan D. M., et al., 2022, Mon. Not. R. Astron. Soc. , 517, 2190

Samus' N. N., Kazarovets E. V., Durlevich O. V., Kireeva N. N., Pastukhova E. N., 2017, Astronomy Reports, 61, 80

Skrutskie M. F., et al., 2006, Astron. J. , 131, 1163

Stassun K. G., et al., 2018, Astron. J. , 156, 102

Whitelock P. A., Feast M. W., Van Leeuwen F., 2008, Mon. Not. R. Astron. Soc. , 386, 313